Association between the renin–angiotensin system and chronic lung allograft dysfunction

Gregory Berra[1,2,10], Sofia Farkona[2,10], Zahraa Mohammed-Ali[2], Max Kotlyar[3], Liran Levy[1,2], Sergi Clotet-Freixas[2], Phillip Ly[1,2], Benjamin Renaud-Picard[1,2], Guan Zehong[1,2], Tina Daigneault[1,2], Allen Duong[1,2], Ihor Batruch[4], Igor Jurisica[3,5], Ana Konvalinka[2,6,7,8,9,11] and Tereza Martinu[1,2,6,8,11]

[1]Toronto Lung Transplant Program, University Health Network, Toronto, ON, Canada. [2]Toronto General Hospital Research Institute, University Health Network, Toronto, ON, Canada. [3]Krembil Research Institute, University Health Network, Toronto, ON, Canada. [4]Dept of Laboratory Medicine and Pathobiology, Lunenfeld-Tanenbaum Research Institute, Mount Sinai Hospital, University of Toronto, Toronto, ON, Canada. [5]Depts of Medical Biophysics and Computer Science, University of Toronto, Toronto, ON, Canada. [6]Multi-Organ Transplant Program, University Health Network, Toronto, ON, Canada. [7]Dept of Medicine, Division of Nephrology, University Health Network, Toronto, ON, Canada. [8]Institute of Medical Science, University of Toronto, Toronto, ON, Canada. [9]Laboratory Medicine and Pathobiology, University of Toronto, Toronto, ON, Canada. [10]G. Berra and S. Farkona contributed equally as first authors. [11]A. Konvalinka and T. Martinu contributed equally as lead authors and supervised the work.

Corresponding author: Ana Konvalinka (ana.konvalinka@uhn.ca)

Shareable abstract (@ERSpublications)
Components of the renin–angiotensin system are increased in chronic lung allograft dysfunction (CLAD) fibrosis. Angiotensin II-regulated proteins in bronchoalveolar lavage identify concurrent and predict future CLAD in lung transplant recipients. https://bit.ly/3eRYez7

Cite this article as: Berra G, Farkona S, Mohammed-Ali Z, *et al*. Association between the renin–angiotensin system and chronic lung allograft dysfunction. *Eur Respir J* 2021; 58: 2002975 [DOI: 10.1183/13993003.02975-2020].

This article has supplementary material available from erj.ersjournals.com

Received: 30 July 2020
Accepted: 6 March 2021

Abstract

Chronic lung allograft dysfunction (CLAD) is the major cause of death after lung transplantation. Angiotensin II (AngII), the main effector of the renin–angiotensin system, elicits fibrosis in both kidney and lung. We identified six AngII-regulated proteins (Ras homolog family member B (RHOB), bone marrow stromal cell antigen 1 (BST1), lysophospholipase 1 (LYPA1), glutamine synthetase (GLNA), thrombospondin 1 (TSP1) and laminin subunit β2 (LAMB2)) that were increased in urine of patients with kidney allograft fibrosis. We hypothesised that the renin–angiotensin system is active in CLAD and that AngII-regulated proteins are increased in bronchoalveolar lavage fluid (BAL) of CLAD patients.

We performed immunostaining of AngII receptors (AGTR1 and AGTR2), TSP1 and GLNA in 10 CLAD lungs and five controls. Using mass spectrometry, we quantified peptides corresponding to AngII-regulated proteins in BAL of 40 lung transplant recipients (stable, acute lung allograft dysfunction (ALAD) and CLAD). Machine learning algorithms were developed to predict CLAD based on BAL peptide concentrations.

Immunostaining demonstrated significantly more $AGTR1^{+}$ cells in CLAD *versus* control lungs ($p=0.02$). TSP1 and GLNA immunostaining positively correlated with the degree of lung fibrosis ($R^2=0.42$ and 0.57, respectively). In BAL, we noted a trend towards higher concentrations of AngII-regulated peptides in patients with CLAD at the time of bronchoscopy, and significantly higher concentrations of BST1, GLNA and RHOB peptides in patients that developed CLAD at follow-up ($p<0.05$). The support vector machine classifier discriminated CLAD from stable and ALAD patients at the time of bronchoscopy (area under the curve (AUC) 0.86) and accurately predicted subsequent CLAD development (AUC 0.97).

Proteins involved in the renin–angiotensin system are increased in CLAD lungs and BAL. AngII-regulated peptides measured in BAL may accurately identify patients with CLAD and predict subsequent CLAD development.

Introduction

Lung transplantation is a life-saving therapy for patients with end-stage lung disease. Despite improvements in early post-operative mortality and long-term outcomes, survival after lung transplant

remains poor compared with other solid organ transplants [1]. Chronic lung allograft dysfunction (CLAD) is the major long-term cause of death after lung transplant, affecting ∼50% of recipients at 5 years post-transplant. Two main clinical CLAD phenotypes, both characterised by fibrosis in different compartments of the lung, have been identified: bronchiolitis obliterans syndrome (BOS), marked by fibrosis within small airways, leading to obstructive pulmonary physiology, and restrictive allograft syndrome (RAS), a more aggressive disease seen in ∼20% of CLAD patients, characterised by diffuse airway and also parenchymal lung fibrosis [2–8]. CLAD mechanisms remain poorly understood and there are no effective treatments. Finding early markers of CLAD and identifying new therapeutic targets represent key goals in lung transplantation.

Acute rejections, infections and environmental exposures drive chronic inflammation and lung allograft injury. The chronic injury, in turn, leads to upregulation of pro-fibrotic mediators, which augment fibroblast proliferation, migration and extracellular matrix (ECM) deposition [9–11]. Studies of tissue fibrogenesis have shown that the "local" renin–angiotensin system mediates fibrosis in multiple organs, including kidney and lung [12–16]. Angiotensin II (AngII), the main effector of the renin–angiotensin system, promotes fibrosis in both kidney and lung [17]. Based on similarities between CLAD fibrosis and kidney allograft interstitial fibrosis and tubular atrophy (IFTA), an important cause of kidney allograft dysfunction and loss, we propose that mechanisms at play in IFTA may also be relevant in CLAD.

We recently identified six AngII-regulated proteins (Ras homolog family member B (RHOB), bone marrow stromal cell antigen 1 (BST1), lysophospholipase 1 (LYPA1), glutamine synthetase (GLNA), thrombospondin 1 (TSP1) and laminin subunit β2 (LAMB2)) in primary kidney cells, and demonstrated that these proteins are dysregulated in kidney grafts with IFTA and increased in urine of IFTA patients [18–20]. For the sake of simplicity, we will be using the protein name to refer to both the protein and respective genes (*RHOB*, *BST1*, *LYPLA1*, *GLUL*, *THBS1* and *LAMB2*) throughout this article. There is evidence that these proteins are associated with, or implicated in, fibrosis in the lung. For instance, TSP1 and LAMB2 were significantly increased in lung tissue from patients with idiopathic pulmonary fibrosis compared with controls [21]. TSP1 catalyses the activation of transforming growth factor (TGF)-β, and is implicated in alveolar macrophage-dependent TGF-β activation in mouse and rat models of bleomycin-induced pulmonary fibrosis [22, 23]. While it is unknown how LAMB2 contributes to idiopathic pulmonary fibrosis pathobiology, it is associated with cell adhesion, differentiation and migration [24], which have all been identified as important factors in fibrogenesis [25, 26]. miR-29, a microRNA involved in LYPA1 regulation [27], is a central rheostat of fibrosis in different organs and model systems [28–31]. More specifically, restoration or overexpression of miR-29 blocked the initiation and progression of fibrosis in mouse lung, kidney and heart *in vivo* [31]. Lastly, BST1 was linked to lung inflammation, radiation fibrosis of the lung [32] and bleomycin-induced fibrosis in mice [33]. To further support our rationale, we built an interactome that shows that these six AngII-regulated proteins are expressed both in kidney and lung, interact closely with the AngII receptors, and are functionally associated with known pro-fibrotic proteins (supplementary material and supplementary figure S1).

Based on the aforementioned available data, we hypothesised that AngII is active in CLAD fibrosis and that AngII-regulated proteins are measurable in bronchoalveolar lavage fluid (BAL) of lung transplant patients as potential markers of CLAD. To test this hypothesis, we sought to determine the expression of AngII receptors (AGTR1 and AGTR2) and AngII-regulated proteins in lung tissue and BAL from CLAD and control patients. We also evaluated whether AngII-regulated proteins in BAL could predict subsequent CLAD development in patients at risk of CLAD.

Patients, materials and methods

Patient selection and sample collection

This study was approved by the University Health Network (Toronto, ON, Canada) Research Ethics Board (protocol 15-9531). Specimens were collected at Toronto General Hospital after written informed consent. The experimental workflow is presented in figure 1. For details, see supplementary material.

Cohort for lung tissue reverse-transcriptase quantitative real-time PCR, immunostaining and Western blotting

CLAD lung tissue was obtained from 33 patients undergoing retransplantation or autopsy between May 2015 and August 2019. CLAD diagnosis and phenotype were adjudicated according the 2019 International Society for Heart and Lung Transplantation consensus [2] by at least two independent reviewers [34]. Control lung tissue was obtained from 10 donor lungs at the end of cold ischaemic time prior to transplantation and from 10 patients undergoing lobar resection for suspected cancer. See figure 2a and supplementary material.

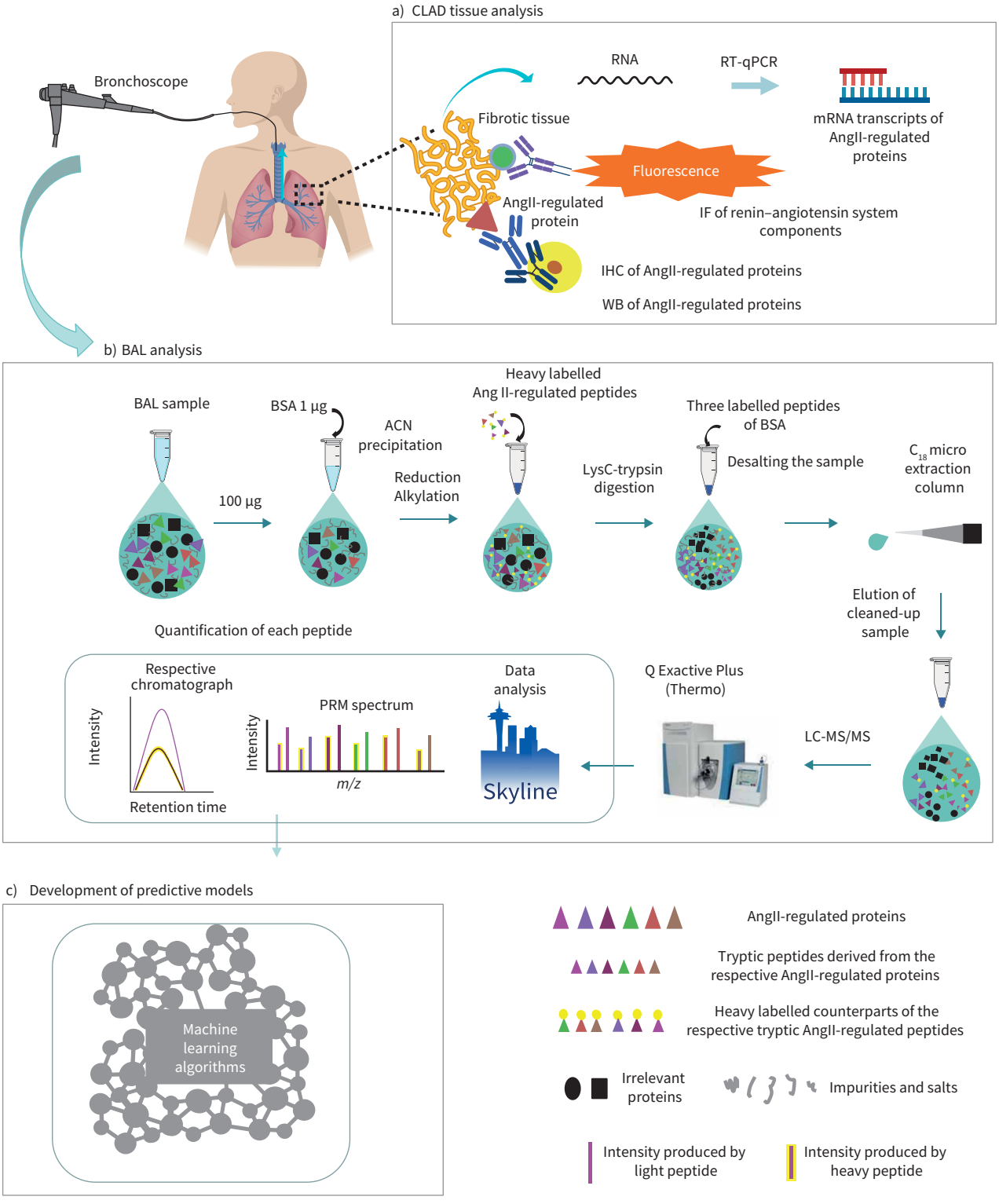

FIGURE 1 Illustration of the experimental workflow. CLAD: chronic lung allograft dysfunction; RT-qPCR: reverse-transcriptase quantitative real-time PCR; AngII: angiotensin II; IF: immunofluorescence; IHC: immunohistochemistry; WB: Western blotting; BAL: bronchoalveolar lavage; BSA: bovine serum albumin; ACN: acetonitrile; heavy labelled: heavy isotope-labelled peptides; LC: liquid chromatography; MS: mass spectrometry; PRM: parallel reaction monitoring. a) mRNA and immunoreactivity of renin–angiotensin system components in CLAD tissue were assessed with RT-qPCR and IF. Immunoreactivity of AngII-regulated proteins in CLAD tissue was evaluated with IHC and IF. AngII-regulated proteins were also assessed by WB. b) Concentrations of AngII-regulated proteins in BAL samples were measured using MS-based targeted assays. Illustration of the steps for quantification of AngII-regulated proteins in human BAL samples using PRM assays. c) Development of predictive models using artificial intelligence.

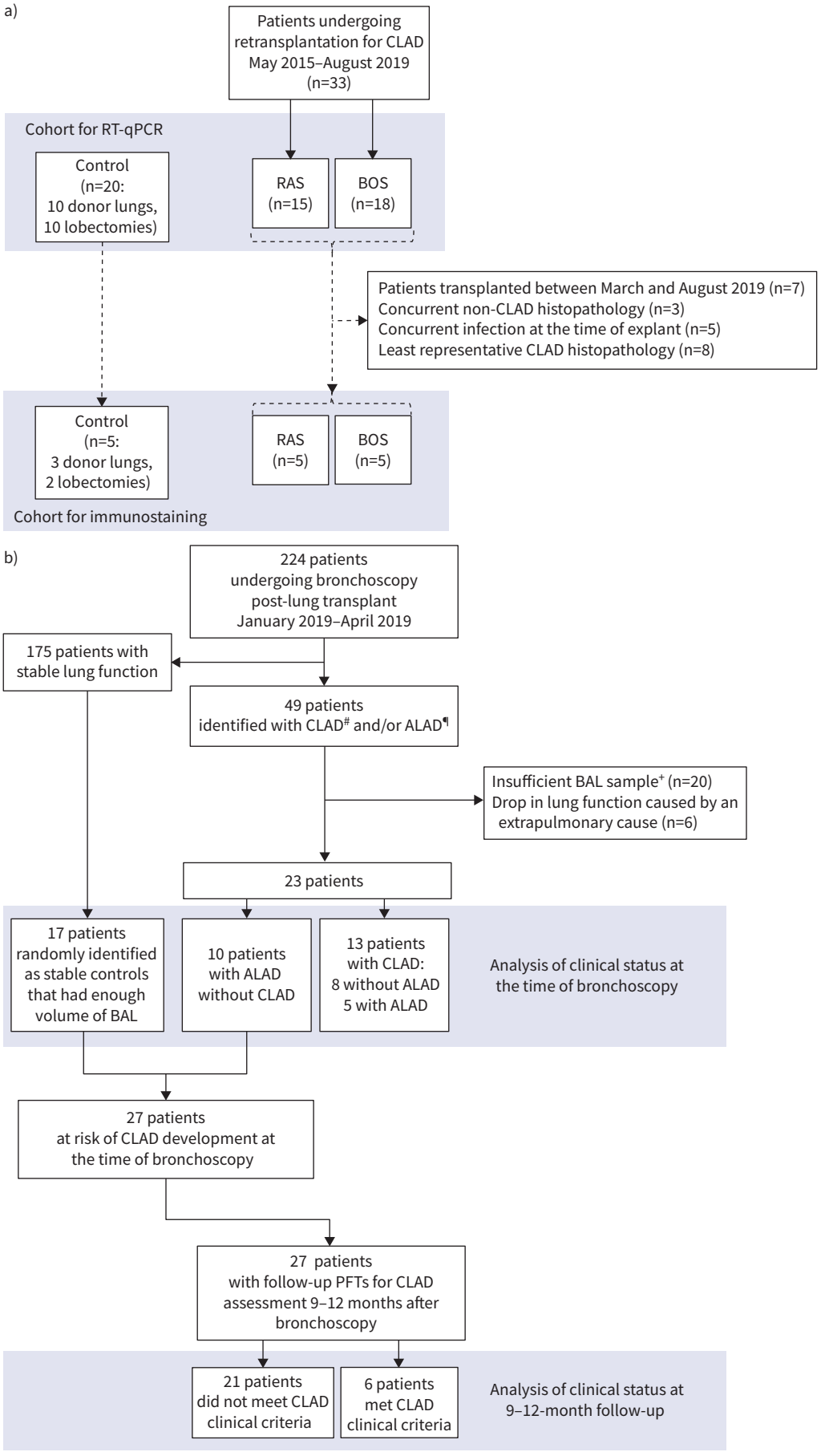
a)
Patients undergoing retransplantation for CLAD May 2015–August 2019 (n=33)
Cohort for RT-qPCR
Control (n=20: 10 donor lungs, 10 lobectomies)
RAS (n=15)
BOS (n=18)
Patients transplanted between March and August 2019 (n=7)
Concurrent non-CLAD histopathology (n=3)
Concurrent infection at the time of explant (n=5)
Least representative CLAD histopathology (n=8)
Control (n=5: 3 donor lungs, 2 lobectomies)
RAS (n=5)
BOS (n=5)
Cohort for immunostaining
b)
224 patients undergoing bronchoscopy post-lung transplant January 2019–April 2019
175 patients with stable lung function
49 patients identified with CLAD# and/or ALAD¶
Insufficient BAL sample+ (n=20)
Drop in lung function caused by an extrapulmonary cause (n=6)
23 patients
17 patients randomly identified as stable controls that had enough volume of BAL
10 patients with ALAD without CLAD
13 patients with CLAD: 8 without ALAD 5 with ALAD
Analysis of clinical status at the time of bronchoscopy
27 patients at risk of CLAD development at the time of bronchoscopy
27 patients with follow-up PFTs for CLAD assessment 9–12 months after bronchoscopy
21 patients did not meet CLAD clinical criteria
6 patients met CLAD clinical criteria
Analysis of clinical status at 9–12-month follow-up

FIGURE 2 Study flow diagrams of the different cohorts. CLAD: chronic lung allograft dysfunction; RT-qPCR: reverse-transcriptase quantitative real-time PCR; RAS: restrictive allograft syndrome; BOS: bronchiolitis obliterans syndrome; ALAD: acute lung allograft dysfunction; BAL: bronchoalveolar lavage; PFT: pulmonary function test; FEV_1: forced expiratory volume in 1 s. a) Study flow of the cohorts used for RT-qPCR and for immunostaining. CLAD lung tissue was obtained from 33 patients between May 2015 and August 2019. The control lungs came from two sources: donor lungs and lobectomy samples. For details, see supplementary material. This cohort of samples was used in its entirety for the RT-qPCR experiments. Immunostaining experiments were performed earlier and therefore included only samples collected up to March 2019. To perform all staining concurrently, we *a priori* limited the number of samples to only those with the most representative bronchiolitis obliterans and pleuroparenchymal fibroelastosis histology, characteristic of BOS and RAS. Three donor lungs and two lung resection control specimens were included as controls for the immunostaining experiments. b) Study flow of the BAL cohort, highlighting the two analyses at the time of bronchoscopy and at follow-up. For this pilot project, we selected only patients who had BAL in excess of what was needed for clinical and biobanking practices at our centre. Of 49 patients with CLAD and/or ALAD, six were excluded because of an extrapulmonary reason for the FEV_1 drop (heart failure, obesity) and 20 had insufficient BAL samples. Of these 20 patients, 17 had insufficient BAL supernatant volumes and three had insufficient protein quantity in the available BAL (<100 µg). #: CLAD is defined according the 2019 International Society for Heart and Lung Transplantation guidelines; ¶: ALAD is defined as an acute drop of FEV_1 ⩾10% compared with the highest FEV_1 in the previous 4 months or the last available FEV_1 before bronchoscopy, if no FEV_1 was available in the preceding 4 months; +: at least 2 mL supernatant remaining after collection for clinical and other competing studies, and at least 100 µg total protein in the sample.

Cohort for BAL protein analysis

This cohort was selected from 224 consecutive lung transplantation patients who underwent a post-lung transplantation surveillance or indication bronchoscopy at our centre between January and April 2019 (bronchoscopy and BAL protocol details are provided in the supplementary material). 20 mL samples of BAL were sent for clinical assessment and any excess was processed for research. After BAL centrifugation at 3220×*g* for 20 min, the supernatant was aliquoted and stored at −80°C. All patients were prospectively screened for CLAD and acute lung allograft dysfunction (ALAD). ALAD was defined as an acute drop in forced expiratory volume in 1 s (FEV_1) ⩾10% compared with the highest FEV_1 in the previous 4 months or the immediately preceding FEV_1 available, in the absence of extrapulmonary causes. 17 control patients with stable lung function were randomly selected from the 175 patients without FEV_1 drop and with sufficient BAL. The concentrations of each peptide and combinations of these peptides were compared between three final groups: 17 stable patients, 10 ALAD patients and 13 CLAD patients (n=40). Of these 40 patients, 27 patients did not have CLAD at the time of bronchoscopy (17 stable patients and 10 ALAD patients). The CLAD status of these 27 patients was reassessed at follow-up, using the last available FEV_1 for each patient obtained 9–12 months after bronchoscopy. See figure 2b and supplementary material.

Analyses of lung tissue and BAL

Paraffin-embedded lung tissue was assessed using haematoxylin/eosin, elastic trichrome and immunostaining for AGTR1, AGTR2, TSP1, GLNA, PanCK, CD45 and α-smooth muscle actin (α-SMA). AGTR1, AGTR2, TSP1, GLNA, LYPA1 and BST1 transcripts were measured using reverse-transcriptase quantitative real-time PCR (RT-qPCR). TSP1 and GLNA protein expression levels were assessed by Western blotting. Targeted mass spectrometry assays were developed to quantify AngII-regulated proteins RHOB, BST1, LYPA1, GLNA, TSP1 and LAMB2 in BAL. Classifiers based on combined peptide concentrations were built using machine learning algorithms, and their diagnostic accuracy and predictive value were assessed in discriminating or predicting CLAD. See figure 1 and supplementary material.

Statistical analyses

Prism version 8.0 (GraphPad, San Diego, CA, USA) was used for the analysis of group characteristics: the t-test or Wilcoxon–Mann–Whitney test was used for continuous variables; the Chi-squared test and Fisher's exact test were used for categorical variables. $p<0.05$ was considered significant.

All other statistical and machine learning analyses were conducted in R version 3.5.1 [35]. Associations between peptide concentrations and patient clinical characteristics were tested: Spearman correlation for continuous variables, Mann–Whitney U-tests for binary patient characteristics and Kruskal–Wallis tests for ordinal patient characteristics. A heatmap of unadjusted p-values was plotted using the ggplot2 3.3.0 package [36]. Peptide concentrations were used to predict CLAD status, using four machine learning

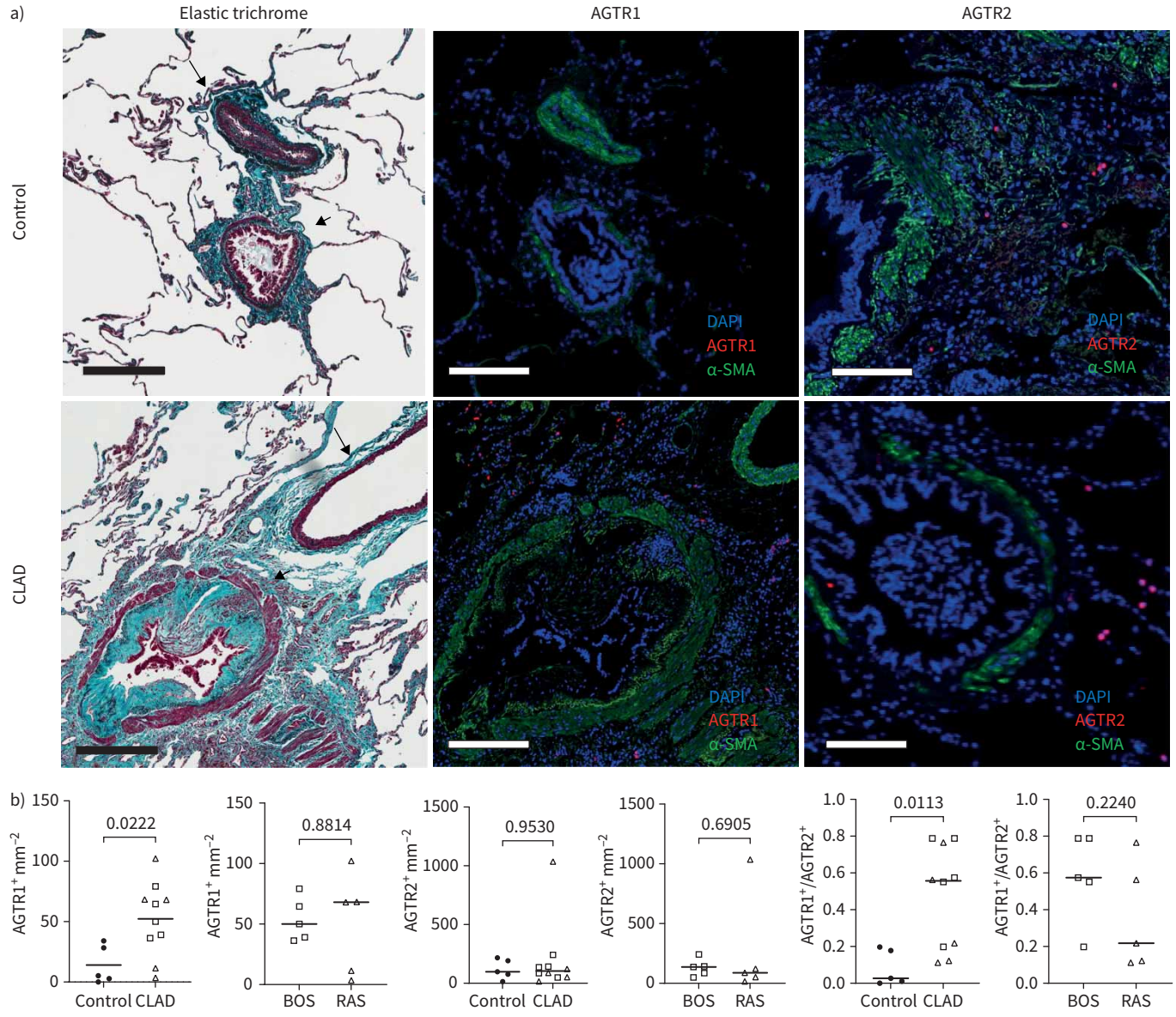

FIGURE 3 Immunofluorescence staining and quantification of renin–angiotensin system components. AGTR1: angiotensin II receptor type 1; AGTR2: angiotensin II receptor type 2; DAPI: 4′,6-diamidino-2-phenylindole; α-SMA: α-smooth muscle actin; CLAD: chronic lung allograft dysfunction; BOS: bronchiolitis obliterans syndrome; RAS: restrictive allograft syndrome. a) Elastic trichrome staining illustration of one airway (short arrow) and its adjacent arteriole (long arrow) in one control and one CLAD sample. The airway in CLAD shows typical obliterative bronchiolitis with peri-airway fibrosis. Immunofluorescence staining of the corresponding zone for AGTR1 and AGTR2. Scale bar: 300 µm. b) Dot plots of the automated quantification by a cytonuclear colocalisation algorithm (supplementary material) of $AGTR1^+$ and $AGTR2^+$ cells in the different groups, with ratio of $AGTR1^+/AGTR2^+$. Each circle, square and triangle represents a patient in the control, BOS and RAS group, respectively, and means and p-values are indicated.

methods (mlr 2.15.0 package [37]): linear discriminant analysis, naïve Bayes, quadratic discriminant analysis and support vector machine (SVM). Predictions were done using leave-one-out cross-validation. Receiver operating characteristic (ROC) curves from predictions were plotted using the pROC 1.15.3 package [38]. p-values of predictions were calculated using the verification 1.42 package [39].

Results

AngII receptors and AngII-regulated proteins and transcripts in explanted CLAD lungs

We analysed AngII receptors (AGTR1 and AGTR2) and AngII-regulated proteins (TSP1 and GLNA) in 33 CLAD and 20 control lungs (figure 2a). CLAD patients had a significantly lower median (interquartile

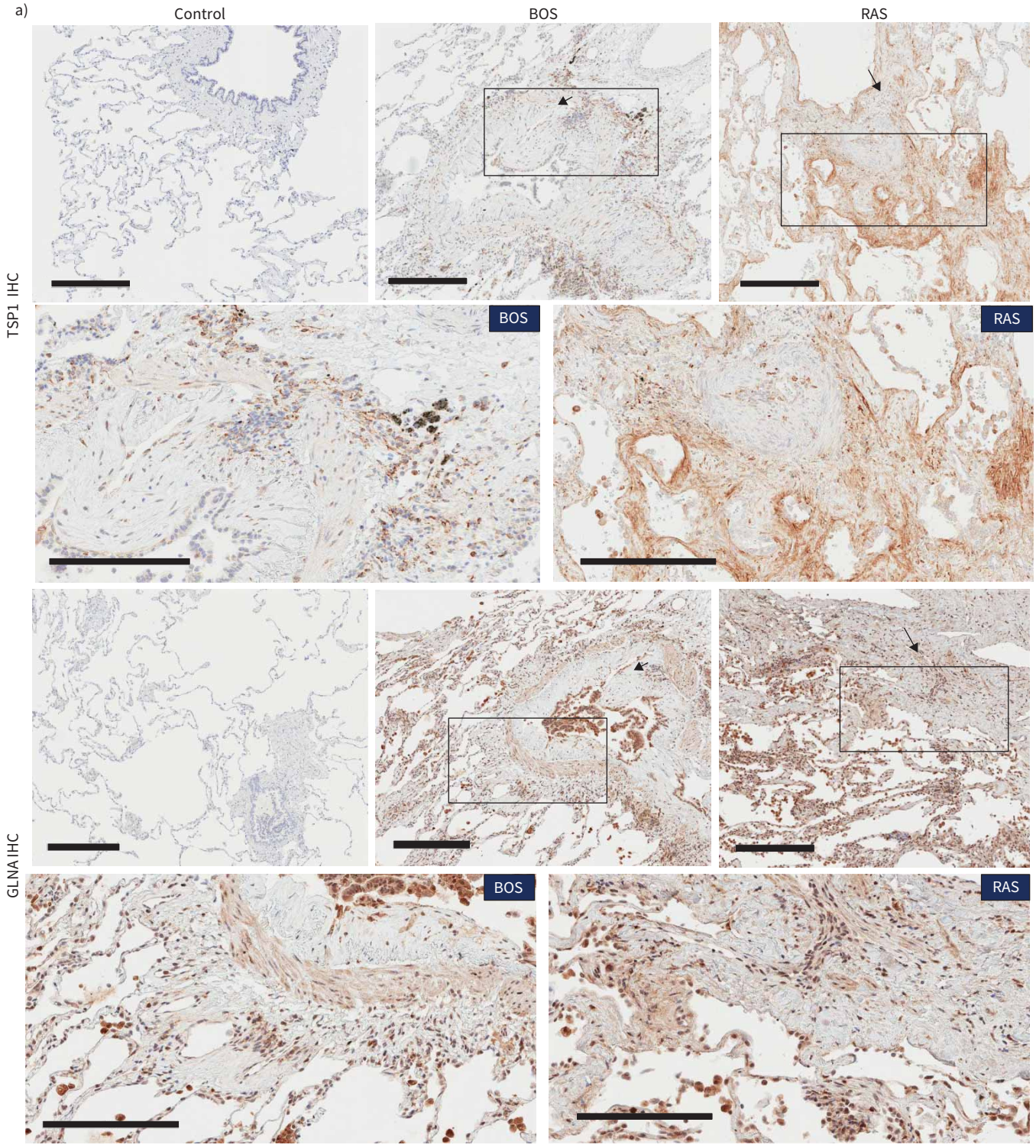

FIGURE 4 Angiotensin II (AngII)-regulated proteins and their transcripts in chronic lung allograft dysfunction (CLAD) *versus* control. BOS: bronchiolitis obliterans syndrome; RAS: restrictive allograft syndrome; IHC: immunohistochemistry; TSP1: thrombospondin 1; GLNA: glutamine synthetase; CLAD: chronic lung allograft dysfunction; PPIA: peptidylprolyl isomerase A. a) IHC staining of TSP1 and GLNA in one control, one BOS and one RAS sample. The images are representative of staining patterns observed in typical obliterative bronchiolitis lesions (short arrows) and parenchymal fibrosis (long arrows). Scale bars: 300 μm (main: rows 1 and 3) and 200 μm (zoom: rows 2 and 4). *Continues on following page.*

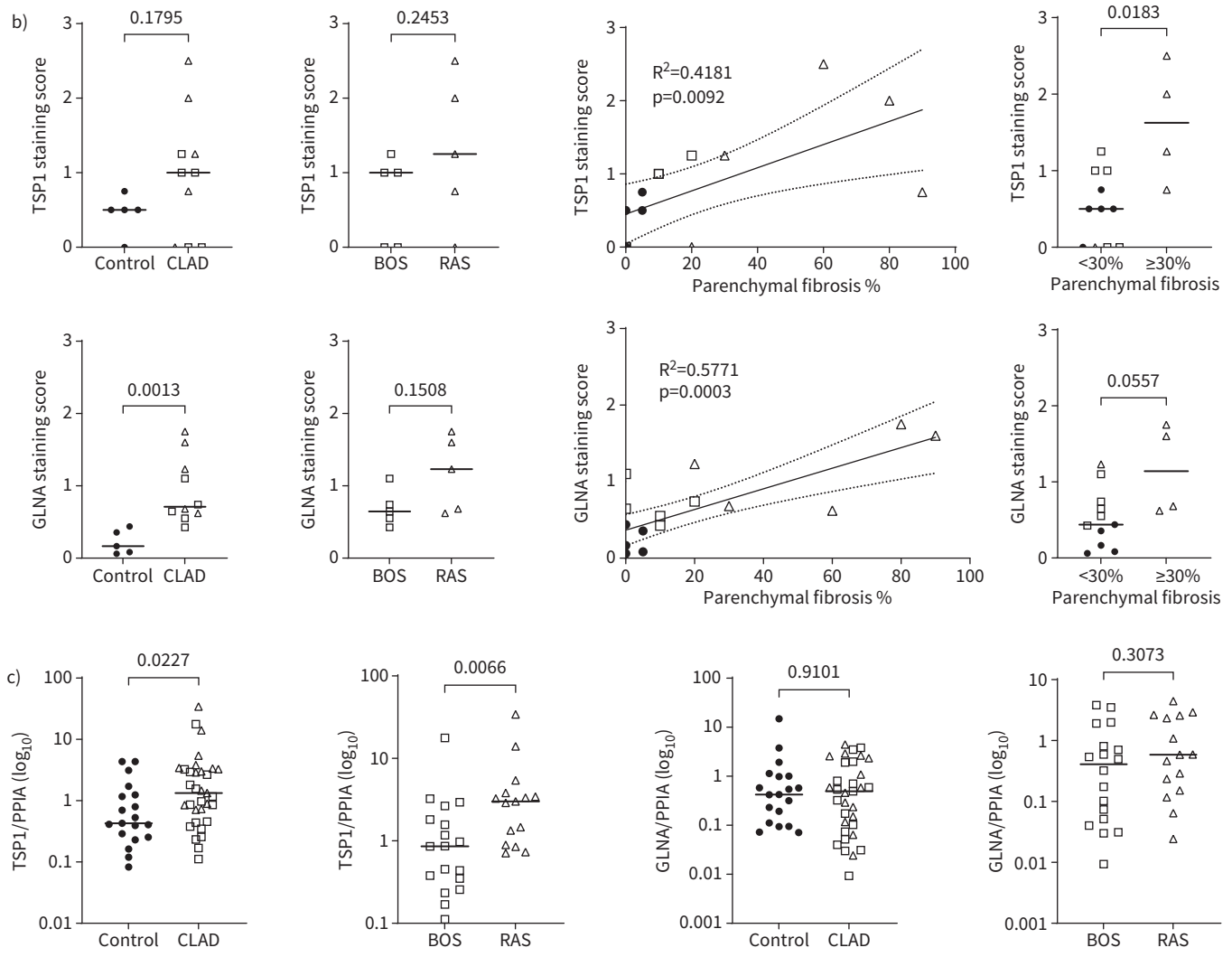

FIGURE 4 *Continued*. b) Dot plots of the overall TSP1 (top) and GLNA (bottom) staining intensity in the different groups, according to the semiquantitative approach described in the supplementary material. The correlations between the extent of parenchymal lung fibrosis (expressed as percentage of the total tissue section) and TSP1 or GLNA staining intensity (R^2=0.42, p=0.01 for TSP1; R^2=0.58, p=0.0003 for GLNA) are shown. Staining intensity for TSP1 (Mann–Whitney test, p=0.02) and GLNA (Mann–Whitney test, p=0.06) is also shown according to the percentage of parenchymal lung fibrosis, categorised as <30% *versus* ⩾30%. c) Transcript levels of TSP1 and GLNA in CLAD *versus* control and in BOS *versus* RAS, normalised by the housekeeping gene for PPIA. In the dot plots, each circle, square and triangle represents a patient in the control, BOS and RAS group, respectively, and means and p-values are indicated.

range (IQR)) age at sample collection (30 (24–48) years) compared with controls (62 (40–68) years), but the lung allograft age was comparable to the age of the control lungs. There was no significant difference in sex or smoking exposure history between CLAD and control patients. Of 33 CLAD specimens, 15 displayed a RAS or mixed phenotype and 18 had a BOS phenotype. Detailed patient characteristics are provided in supplementary table S1. The cohort used for immunostaining is a subset of the RT-qPCR cohort, with similar clinical characteristics as the larger RT-qPCR cohort (supplementary table S2).

As evident from trichrome staining, CLAD lungs had higher ECM deposition compared with controls (figure 3a). Quantification of immunostaining demonstrates significantly higher numbers of $AGTR1^+$ cells in CLAD compared with controls (unpaired t-test, p=0.022). There was no difference in the mean number of $AGTR1^+$ cells in BOS *versus* RAS (figure 3b and supplementary figure S2). Moreover, the mean number of $AGTR2^+$ cells was not significantly different in CLAD *versus* controls or in BOS *versus* RAS (figure 3b). Quantifying the staining as the percentage of the total number of cells did not affect the results (supplementary figure S3). Finally, the AGTR1/AGTR2 ratio was significantly higher in CLAD *versus*

TABLE 1 Baseline patient and bronchoscopy-based characteristics of patients according their clinical status at the time of bronchoscopy

	Stable	ALAD	CLAD	p-value
Patients	17	10	13	
Patient characteristics				
Recipient age at transplant years	65 (41.5–72)	65 (58–70.3)	62 (24.5–72)	0.77
Male	12 (70.6)	6 (60.0)	9 (69.2)	0.84
Native lung disease				0.15
Pulmonary fibrosis	7 (41.2)	4 (40.0)	6 (46.1)	
COPD	5 (29.4)	3 (30.0)	4 (30.8)	
Cystic fibrosis	4 (23.5)	0 (0)	3 (23.1)	
Others[#]	1 (5.9)	3 (30.0)	0 (0)	
Transplant type				0.91
Double lung[¶]	13 (76.5)	7 (70.0)	10 (76.9)	
Donor (D)/recipient (R) CMV mismatch status				0.59
D+/R−	4 (23.6)	1 (10.0)	1 (7.7)	
D+/R+ and D−/R+	10 (58.8)	8 (80.0)	8 (61.5)	
D−/R−	3 (17.6)	1 (10.0)	4 (30.8)	
Donor characteristics				
Age of donor at transplant years	42.6±15.7	46±13.9	48.6±22	0.67
Ever-smoker	11 (64)	4 (40.0)	3 (23)	0.05
Pack-years	10 (4–20)	9 (2.8–13)	2 (one value)	0.67
Time from CLAD onset to bronchoscopy days			137 (82–371)	
Bronchoscopy-based characteristics				
Time from transplant to bronchoscopy days	270 (181–550)	202 (181–366)	571 (363–1407)	0.005*
Presence of respiratory symptoms				0.00002*
Acute symptoms (<1 month)	2 (11.8)	6 (60.0)	7 (54)	
Chronic (>1 month)	0 (0)	2 (20.0)	4 (31)	
Last available FEV_1 before bronchoscopy				
Mean±SD absolute FEV_1 L	2.39±0.93	1.68±0.65	1.57±0.64	0.014*
Median drop from CLAD baseline %	−5.4	−20.5	−29.7	<0.0001*
Median drop from ALAD baseline %	0	−19.7	−8.3	<0.0001*
CMV PCR				0.25
None measured	2 (11.8)	0 (0)	2 (15.4)	
None detected or below quantification threshold	14 (88.2)	8 (80.0)	8 (61.6)	
Positive	1 (5.9)	2 (20.0)	3 (23)	
Immunosuppressive treatment				
Cyclosporine/tacrolimus	13/4	8/2	6/7	0.13
Prednisone dose $mg \cdot day^{-1}$	12.5 (10–20)	15 (14.3–18.1)	10 (6.3–17.5)	0.19
Prior AR treatment within 3 months	3	0	2	0.38
Renin–angiotensin system blocking agents				0.4787
Patients on blocking agent[+]	3 (17.6)	4 (40.0)	3 (23.1)	
ACE inhibitor prescription	2/3 (66.7)	1/4 (25.0)	3/3 (100)	
AngII receptor blocker prescription	1/3 (33.3)	3/4 (75.0)	0/3 (0)	
Lung opacities on chest CT scan				0.27
No significant abnormalities	10	3	4	
Acute abnormalities	5	4	5	
Chronic abnormalities	2	5	3	
A grade				0.45
A0	7 (41.2)	5 (50.0)	5 (38.5)	
⩾A1	1 (5.9)	1 (10.0)	1 (7.7)	
AX	7 (41.2)	2 (20.0)	2 (15.3)	
Biopsy not performed	2 (11.7)	2 (20.0)	5 (38.5)	
B grade				0.48
B0	2 (11.8)	1 (10.0)	2 (15.3)	
BX	13 (76.4)	7 (70.0)	6 (46.2)	
Biopsy not performed	2 (11.8)	2 (20.0)	5 (38.5)	
AR treatment introduced after bronchoscopy	1[§] (5.9)	1 (10.0)	4 (30.8)	0.20
BAL cytology analysis				0.83
Acute inflammation	2 (11.8)	4 (40.0)	3 (23.1)	
Chronic inflammation	2 (11.8)	1 (10.0)	1 (7.7)	
Eosinophilic inflammation	1 (5.9)	0 (0)	2 (15.3)	

Continued

TABLE 1 Continued

	Stable	ALAD	CLAD	p-value
Significant bacterial pathogens in BAL	2[f] (11.8)	0 (0)	2[##] (15.3)	0.45
Initiation of antimicrobial treatment post-bronchoscopy	4 (23.6)	4 (40.0)	4 (30.8)	0.66
With microbiological documentation of a significant pathogen in BAL	2 (11.8)	0 (0)	1 (7.7)	
Without microbiological documentation of a significant pathogen	2 (11.8)	4 (40.0)	3 (23.1)	

Data are presented as n, median (interquartile range) for non-normally distributed variables, n (%) or mean±SD for normally distributed variables, unless otherwise stated. Distribution of demographic characteristics was tested by the Kolmogorov–Smirnov test. ALAD: acute lung allograft dysfunction; CLAD: chronic lung allograft dysfunction; COPD: chronic obstructive pulmonary disease; CMV: cytomegalovirus; FEV_1: forced expiratory volume in 1 s; AR: acute rejection; ACE: angiotensin converting enzyme; AngII: angiotensin II; CT: computed tomography; BAL: bronchoalveolar lavage. [#]: one patient had pulmonary arterial hypertension in the stable group, and one patient had lymphangioleiomyomatosis and two patients had bronchiectasis in the ALAD group; [¶]: all the other patients were single lung transplant (no patient with heart and lung transplant was included); [+]: significant prescription was defined as a continuous prescription for at least 4 weeks; [§]: patient already treated for persistent A2 rejection at time of bronchoscopy (introduction of intravenous immunoglobulin for antibody-mediated rejection component after bronchoscopy); [f]: *Pseudomonas aeruginosa* and *Haemophilus influenzae*; [##]: *P. aeruginosa* and *Mycobacterium avium* (first isolation without any corresponding clinical and radiological context: no treatment introduced). For comparison between the three groups, we used one-way ANOVA or nonparametric equivalent. Proportions of discrete variables were assessed by the Chi-squared test and Fischer's exact test. *: p<0.05.

controls but not in BOS *versus* RAS (figure 3b). Both AGTR1 and AGTR2 co-stained with CD45, but not with α-SMA or PanCK (supplementary figure S4).

Surprisingly, AGTR1 gene expression was 4 times higher in controls compared with CLAD lungs (Mann–Whitney test, p<0.05). In contrast, AGTR2 transcript levels tended to be higher in CLAD than in controls (Mann–Whitney test, p=0.07). There were no statistically significant differences in AGTR1 or AGTR2 transcript levels between BOS and RAS (supplementary figures S5–S7).

TSP1 and GLNA staining was assessed in the same cohort of CLAD and control lungs (figure 4a, and supplementary figures S8 and S9). Positive TSP1 staining was identified in areas of dense fibrosis. Cells in the alveolar regions stained positively for both TSP1 and GLNA. We noted a statistically higher immunoreactivity of GLNA in CLAD *versus* controls (Mann–Whitney test, p<0.0013), and consistent trends towards higher staining of TSP1 in CLAD *versus* controls and of both GLNA and TSP1 in RAS *versus* BOS lungs (figure 4b). TSP1 (p=0.03) and GLNA (p=0.20) protein expression levels (supplementary material) were higher in the RAS cases compared with controls by Western blotting (supplementary figure S10). Immunofluorescence for TSP1 and GLNA showed coexpression with CD68 (monocyte/macrophage marker) (supplementary figure S11).

We found a significant positive correlation between AngII-regulated proteins TSP1 and GLNA and the extent of parenchymal fibrosis in each CLAD specimen, estimated by blinded histological scoring (figure 4b, supplementary material and supplementary figure S12). When dividing the patients into two groups based on fibrosis extent, higher TSP1 and GLNA immunoreactivity was identified in patients with ⩾30% parenchymal fibrosis (figure 4b).

TSP1 gene expression was significantly higher in CLAD compared with control lungs (Mann–Whitney test, p=0.02) and in RAS compared with BOS (Mann–Whitney test, p=0.006) (figure 4c). GLNA, LYPA1 and BST1 transcripts were similar in CLAD *versus* controls and in BOS *versus* RAS lungs (figure 4c, and supplementary figures S6, S7 and S13).

Quantification of AngII-regulated proteins in BAL of lung transplant recipients

Baseline patient characteristics at the time of bronchoscopy were comparable between stable, ALAD and CLAD patients (table 1).

Using optimised parallel reaction monitoring (PRM) assays (supplementary figures S14 and S15), we detected two native peptides of TSP1, BST1, GLNA and LYPA1 protein and one RHOB peptide in a pool of BAL from controls and CLAD patients. We constructed linearity curves (supplementary figure S16) for BST1, GLNA, LYPA1 and RHOB. LAMB2 protein was not detected in BAL. TSP1 was detected in the pooled BAL, but at levels which would not make the quantification confident.

We then quantified AngII-regulated peptides in individual BAL samples. First, we examined whether AngII-regulated peptide concentrations correlated with clinical characteristics at the time of bronchoscopy

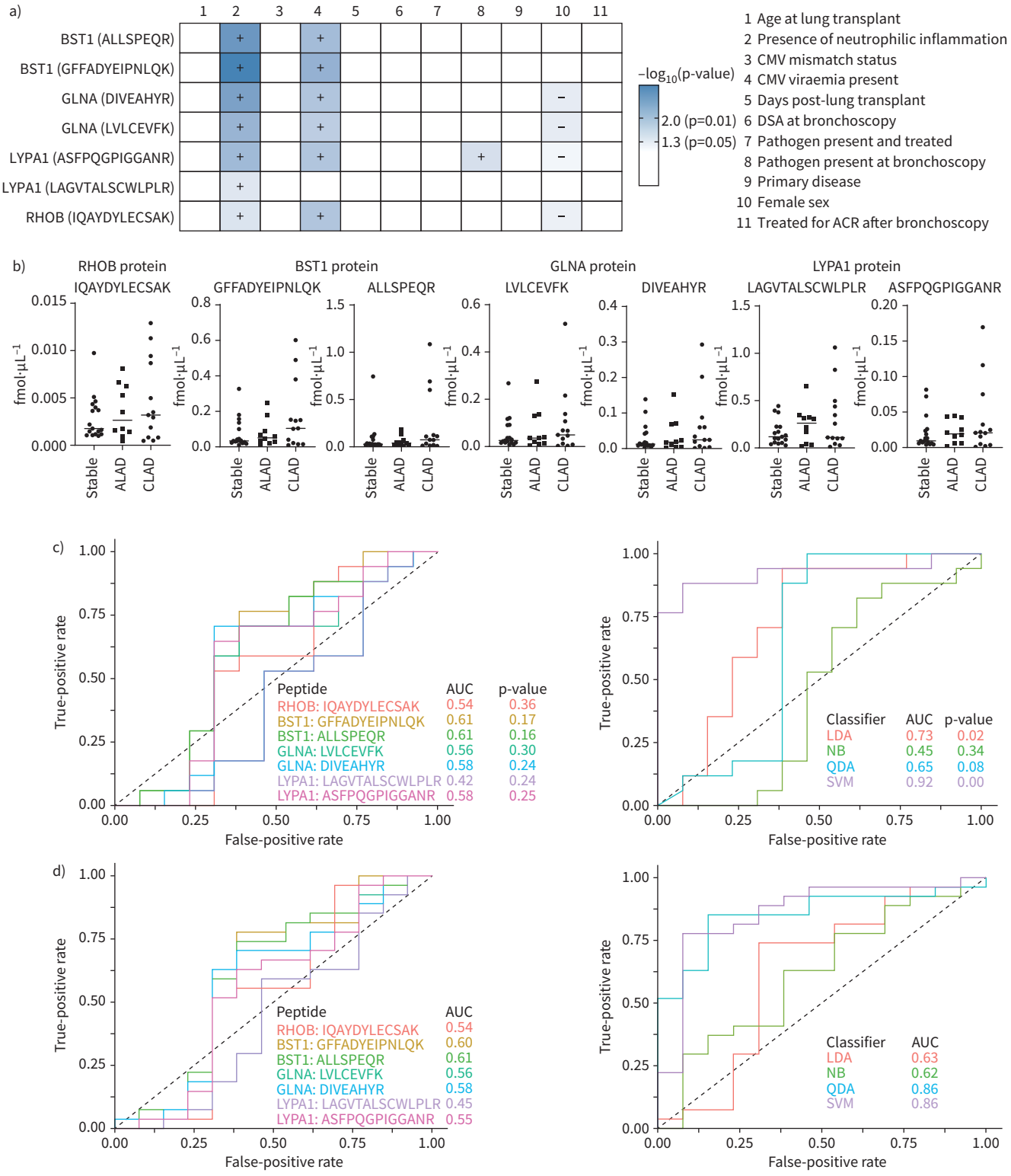

FIGURE 5 Concentration of angiotensin II (AngII)-regulated peptides in bronchoalveolar lavage (BAL) and clinical status at the time of bronchoscopy. BST1: bone marrow stromal cell antigen 1; GLNA: glutamine synthetase; LYPA1: lysophospholipase 1; RHOB: Ras homolog family member B; CMV: cytomegalovirus; DSA: donor-specific antibody; ACR: acute cellular rejection; ALAD: acute allograft dysfunction; CLAD: chronic lung allograft dysfunction; AUC: area under the curve; LDA: linear discriminant analysis; NB: naïve Bayes; QDA: quadratic discriminant analysis; SVM: support vector machine. a) Heatmap showing the association between patient clinical characteristics at the time of bronchoscopy and the concentration of AngII-regulated peptides. Blue indicates significant p-values (Spearman correlation for continuous variables, Mann–Whitney U-tests for binary patient characteristics and Kruskal–Wallis tests for ordinal patient characteristics, p<0.05), with darker colour indicating lower

p-value. "+" indicates that the presence of the clinical characteristic is associated with higher peptide concentrations; "–" indicates that the presence of the clinical characteristic is associated with lower peptide concentrations. b) Plots of the concentration of seven AngII-regulated peptides from RHOB, BST1, GLNA and LYPA1 proteins, according to patient clinical status at the time of bronchoscopy: stable, ALAD and CLAD. c, d) Receiver operating characteristic curves showing the performance of each individual peptide (on the left) or different machine learning algorithms combining the seven peptides (on the right) for c) detection of CLAD *versus* stable patients at the time of bronchoscopy and d) prediction of CLAD *versus* no CLAD at the time of bronchoscopy.

(figure 5a). AngII-regulated peptide concentrations correlated significantly and directly with the degree of neutrophilic inflammation and cytomegalovirus (CMV) viraemia. GLNA, RHOB and LYPA1 peptides also correlated with the recipient's sex. Importantly, there was no correlation between the peptide concentrations and the time elapsed between transplantation and BAL collection.

Second, we compared AngII-regulated peptides between patient groups, based on the presence of CLAD or ALAD at the time of bronchoscopy. Although a trend was observed for higher concentrations of RHOB, BST1 and GLNA peptides in BAL from CLAD patients compared with the other two groups, this difference was not statistically significant (figure 5b). We then examined whether the concentrations of individual peptides and combinations of the seven peptides using machine learning approaches could segregate patient groups. Individual peptide concentrations were marginally better compared with chance alone (figure 5c). However, the SVM classifier accurately discriminated CLAD from stable patients with area under the curve (AUC) 0.92 (figure 5c). The SVM classifier also discriminated between CLAD and no CLAD (stable+ALAD) with AUC 0.86 (figure 5d).

We wondered whether AngII-regulated protein concentrations in BAL could predict development of CLAD in the subsequent 12 months. We thus focused on the 27 patients in the BAL cohort who did not have a diagnosis of CLAD at the time of bronchoscopy, but who had a subsequent 9–12-month follow-up FEV_1 (figure 2b). The baseline clinical and bronchoscopy-based characteristics were largely comparable between patients who developed CLAD at follow-up (n=6) and patients who did not (n=21) (table 2).

Concentrations of RHOB, BST1 and GLNA peptides (IQAYDYLECSAK, GFFADYEIPNLQK, ALLSPEQR and LVLCEVFK) at the time of bronchoscopy were significantly higher in patients who developed CLAD at follow-up compared with those who did not (figure 6a). We noted a consistent trend in the same direction for the remaining peptides. We then examined the ability of individual or combined peptide concentrations to predict CLAD development using machine learning. Individual peptide concentrations had a modest-to-good accuracy with AUC 0.58–0.80 (figure 6b). The SVM classifier that included combined peptide concentration had excellent accuracy with AUC 0.97 in predicting subsequent CLAD development (figure 6b).

Discussion

We examined the presence of AngII receptors and our previously reported AngII-regulated proteins in CLAD lungs, and measured the concentration of AngII-regulated proteins in BAL from lung transplantation recipients. We made three major observations: 1) AngII receptor AGTR1 is increased in CLAD *versus* control lungs and AngII-regulated proteins TSP1 and GLNA correlate with the degree of lung fibrosis; 2) classifiers based on combined AngII-regulated peptides measured in BAL accurately distinguish CLAD from stable and ALAD patients; and 3) AngII-regulated peptides in BAL predict CLAD development.

Applying immunofluorescence, we found significantly higher numbers of $AGTR1^+$ cells, with a higher ratio of $AGTR1^+/AGTR2^+$ cells in CLAD. The renin–angiotensin system plays an important role in fibrosis of the lung and other organs, and this system may have an instrumental role in CLAD. Pre-clinical and clinical studies showed that the renin–angiotensin system and its main effector AngII are active in lung fibrosis [40–45]. These deleterious effects can be reversed by renin–angiotensin system inhibitors in mice [40]. AGTR1 is the mediator of pro-fibrotic and pro-inflammatory effects of AngII [44]. A consistently higher expression of AGTR1 has been shown in fibrotic lung conditions [15, 16, 41, 42]. In contrast, AGTR2 is thought to have more modulatory effects [15, 44]. While both AGTR1 and AGTR2 increase during wound healing [46], existing data on AGTR2 expression in different fibrotic conditions are conflicting [47]. Surprisingly and contrary to the protein levels, transcript levels of AGTR1 were lower and transcript levels of AGTR2 were higher in CLAD. While we have no definitive explanation for this observation, we formulate several hypotheses. First, CLAD samples displayed advanced fibrosis, where active transcription may have been reduced. Downregulation of AngII receptor transcripts in advanced

TABLE 2 Characteristics of patients at risk of chronic lung allograft dysfunction (CLAD) at the time of bronchoscopy according to their status at follow-up

	Clinical status at follow-up		p-value
	Remaining stable	Developing CLAD	
Patients	21	6	
Patient characteristics			
Recipient age at transplant years	65 (41.5–72)	63.5 (58–68)	0.89
Male	13 (61.9)	5 (83.3)	0.63
Native lung disease			0.69
Pulmonary fibrosis	9 (42.9)	2 (33.3)	
COPD	5 (23.8)	3 (50.0)	
Cystic fibrosis	4 (19.0)	0 (0)	
Others	3 (14.3)	1 (16.7)	
Transplant type			>0.99
Single lung	6 (28.6)	1 (16.7)	
Double lung	15 (71.4)	5 (83.3)	
Donor (D)/recipient (R) CMV mismatch status			0.08
D+/R−	13 (61.9)	1 (16.7)	
D+/R+ and D−/R+	4 (19.0)	5 (83.3)	
D−/R−	4 (19.0)	0 (0)	
Donor characteristics			
Age of donor at transplant years	45.2±14.3	39.3±17.4	0.41
Ever-smoker	11 (52.4)	4 (66.7)	0.66
Pack-years	10 (6.5–16.5)	7.5 (1–18.5)	0.77
EVLP before implantation of organ	11 (52.4)	3 (50.0)	>0.99
Time from bronchoscopy to CLAD onset days		119.8±135.6	
Bronchoscopy-based characteristics			
Time post-transplant days	268 (180–369)	287.5 (213–750)	0.23
Presence of respiratory symptoms			
Acute symptoms (<1 month)	5 (23.8)	3 (50.0)	0.32
Chronic (>1 month)	1 (4.8)	1 (16.7)	0.40
Last available FEV_1 before bronchoscopy			
Mean±SD absolute FEV_1 L	2.2 (0.95)	1.9 (0.67)	0.46
Mean±SD drop from CLAD baseline %	−9.57±9.46	−14.6±10.98	0.27
Mean±SD drop from ALAD baseline %	−7.58±10.29	−9.02±12.65	0.77
CMV PCR			0.12
None measured	2 (9.5)	0 (0)	
None detected	18 (85.7)	4 (66.7)	
Positive	1 (4.8)	2 (33.3)	
Immunosuppressive regimen			
Cyclosporine/tacrolimus	16/5	5/1	0.71
Prednisone dose $mg \cdot day^{-1}$	15 (10–20)	13.75 (11.25–16.25)	0.86
Prior AR treatment within 1 month	1	0	0.59
Prior AR treatment within 3 months	2	0	0.43
Renin–angiotensin system blocking agent			0.28
Patients on blocking agent	4 (19.0)	3 (50.0)	
ACE inhibitor prescription	1 (4.8)	2 (33.3)	
AngII receptor blocker prescription	3 (14.2)	1 (16.7)	
Lung opacities on chest CT scan			
No significant abnormalities	12 (57.1)	1 (16.7)	0.17
Acute abnormalities	6 (28.6)	3 (50.0)	0.37
Chronic abnormalities	4 (19.0)	3 (50.0)	0.29
Current DSAs	6 (28.6)	1 (16.7)	>0.99
A grade			0.22
A0	8 (38.1)	4 (66.7)	
A1	1 (4.8)	0 (0)	
A2	1 (4.8)	0 (0)	
AX	9 (42.9)	0 (0)	
Biopsy not performed	2 (9.5)	2 (33.3)	
B grade			0.96
B0	2 (9.5)	1 (16.7)	

Continued

TABLE 2 Continued

	Clinical status at follow-up		p-value
	Remaining stable	Developing CLAD	
B1R	0 (0)	0 (0)	
B2R	0 (0)	0 (0)	
BX	17 (80.1)	3 (50.0)	
Biopsy not performed	2 (9.5)	2 (33.3)	
AR treatment introduced after bronchoscopy	2 (9.5)	0 (0)	>0.99
BAL cytology analysis			
Acute inflammation	3 (14.3)	2 (33.3)	0.30
Chronic inflammation	0 (0)	2 (33.3)	0.04*
Eosinophilic inflammation	1 (4.8)	0 (0)	>0.99
Other pathological abnormalities on transbronchial biopsies			
Haemosiderosis	2 (9.5)	0 (0)	>0.99
Organising pneumonia	0 (0)	1 (16.7)	0.22
Interstitial chronic inflammation	9 (42.9)	3 (50.0)	>0.99
Antimicrobial treatment at time of bronchoscopy			
New antimicrobial treatment initiated post-bronchoscopy	6 (28.6)	1 (16.7)	>0.99
With microbiological documentation	2 (9.5)	1 (16.7)	0.55
Pre-existent treatment	3 (14.3)	1 (16.7)	>0.99
BAL microbiology result			
Significant bacterial pathogens	1 (4.8)	1 (16.7)	0.40
Significant viral pathogens	0 (0)	0 (0)	>0.99
Significant fungal pathogens	3 (14.3)	0 (0)	>0.99
Galactomannan positive	0 (0)	0 (0)	>0.99

Data are presented as n, median (interquartile range) for non-normally distributed variables, n (%) or mean±SD for normally distributed variables, unless otherwise stated. Distribution of demographic characteristics was tested by the Kolmogorov–Smirnov test. COPD: chronic obstructive pulmonary disease; CMV: cytomegalovirus; EVLP: *ex vivo* lung perfusion; FEV_1: forced expiratory volume in 1 s; AR: acute rejection; ACE: angiotensin converting enzyme; AngII: angiotensin II; CT: computed tomography; DSA: donor-specific antibody; BAL: bronchoalveolar lavage. Comparison of mean or median of continuous variables in two groups was assessed by the t-test or Mann–Whitney test, respectively. Proportions of discrete variables were assessed by the Chi-squared test and Fischer's exact test. *: p<0.05.

fibrosis was shown previously [48]. Second, AngII receptor activation, *via* a negative feedback loop, may induce transcriptional downregulation, perhaps through the β-arrestin pathway [49]. Treatment of mesangial cells with AngII markedly suppressed AGTR1 mRNA expression [50]. Third, NF-κB inhibition by calcineurin inhibitors in lung transplant recipients downregulates AGTR1 transcription [51]. We next examined the cell types expressing AngII receptors and found positive co-staining for both AGTR1 and AGTR2 with $CD45^+$ cells, suggesting the expression of AngII receptors by immune cells, as previously reported [52–54].

Among AngII-regulated proteins, GLNA displayed higher immunostaining, while TSP1 displayed a trend towards an increase in CLAD. Their immunostaining correlated with the extent of parenchymal fibrosis within CLAD lungs. Furthermore, RT-qPCR analysis showed significantly higher TSP1 expression in CLAD. TSP1 is a structural and regulatory ECM glycoprotein [55]. TSP1 mediates kidney fibrosis *in vitro* [56] and *in vivo* [57, 58], and has been linked to ischaemia reperfusion injury and fibrosis in kidney allografts in both animal models and patients [59–61]. Finally, TSP1 mRNA levels were significantly increased in urine cell pellets from kidney transplant patients with fibrosis (IFTA) compared with controls [62], while TSP1 urine protein excretion was significantly increased in IFTA [20]. GLNA is the ATP-dependent enzyme that catalyses the synthesis of glutamine from glutamate and ammonia. GLNA is required for proliferation of fetal skin fibroblasts, and is expressed in fibroblasts and immune cells of the tumour micro-environment. GLNA differential expression had been used to monitor regression of fibrosis in hepatic injury [63]. The other AngII-regulated proteins that we examined in lung tissue and monitored in BAL have also been involved in fibrosis. BST1 gene knockout protects against fibrosis in a mouse model of renal ischaemia reperfusion injury [64]. RHOB belongs to a family of GTPases upregulated by TGF-β and is involved in actin cytoskeleton remodelling in fibroblasts [65, 66]. LYPA1 protein is involved in nitric oxide metabolism. MIR29B1 gene mutation resulted in significantly increased fibrosis and LYPA1 protein expression and lower nitric oxide in the renal outer medulla in rats [27]. These AngII-regulated proteins thus participate in fibrosis, although it remains unclear if they are controlled by a common regulator, downstream of AGTR1.

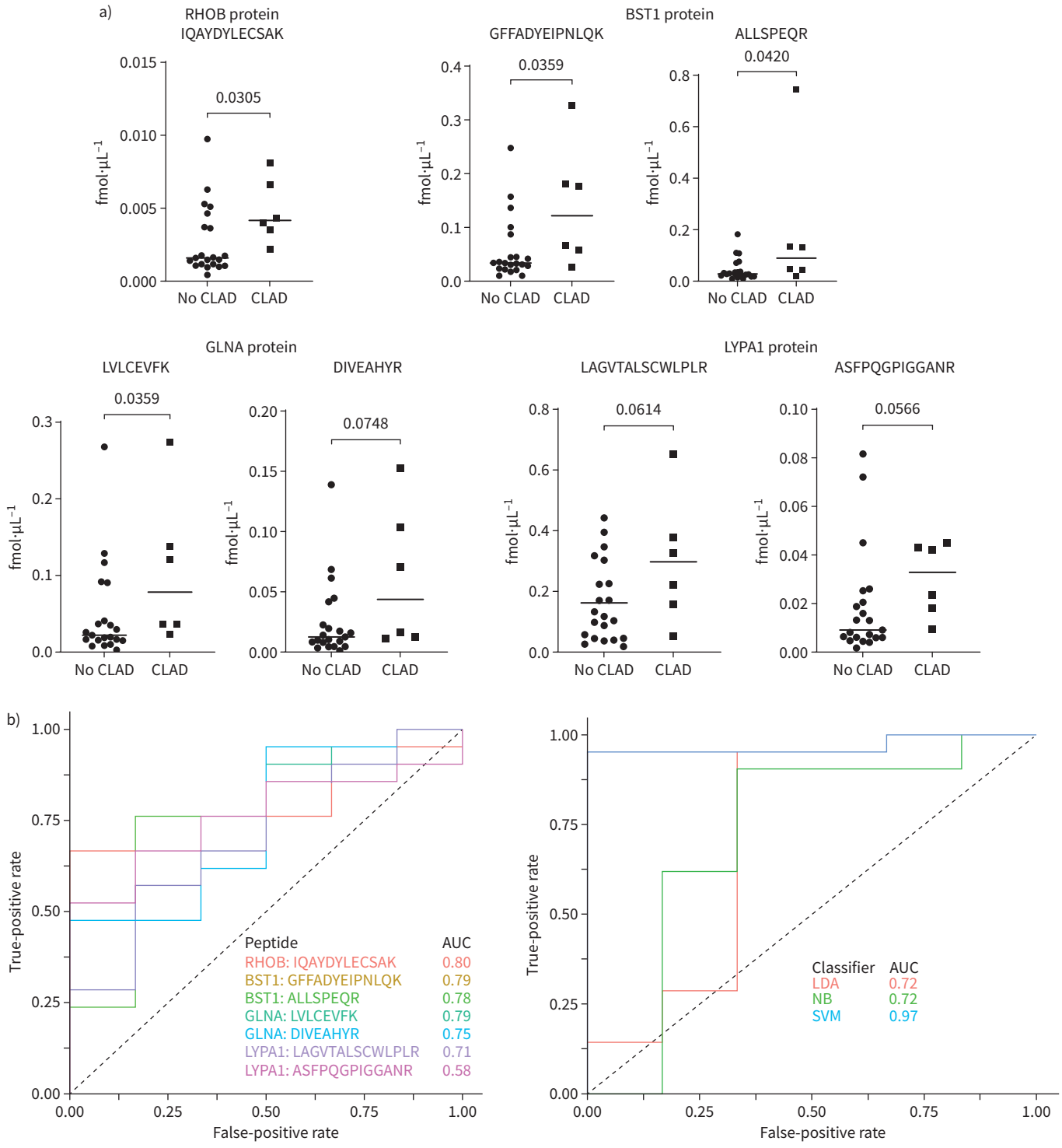

FIGURE 6 Concentration of angiotensin II (AngII)-regulated proteins in bronchoalveolar lavage (BAL) and subsequent development of chronic lung allograft dysfunction (CLAD). RHOB: Ras homolog family member B; BST1: bone marrow stromal cell antigen 1; GLNA: glutamine synthetase; LYPA1: lysophospholipase 1; AUC: area under the curve; LDA: linear discriminant analysis; NB: naïve Bayes; SVM: support vector machine. a) Plots of the concentration of two peptides for each AngII-regulated protein (BST1, GLNA and LYPA1) and one peptide for RHOB. The normality of the distribution of the peptide concentrations at follow-up was assessed with the Kolmogorov–Smirnov test. The comparison of the concentration of each peptide according to the follow-up clinical status (CLAD development and no CLAD development) was performed with the t-test or Mann–Whitney test according to the distribution. b) Performance of each peptide individually (left) and performance of different machine learning algorithms (right) combining seven peptides for prediction of CLAD status (CLAD *versus* no CLAD) at follow-up.

For the measurement of the AngII-regulated proteins in BAL samples, we developed PRM assays that selectively monitor peptides unique to our proteins. PRM assays are highly selective, are cost-effective due to their multiplexing capabilities [67, 68] and are suggested for proteins for which no high-quality antibodies have been generated [69]. The limitation of PRM is poor sensitivity for very low abundance proteins in a complex matrix. Our PRM assays showed good performance for quantification of four out of six AngII-regulated proteins, *i.e.* BST1, GLNA, LYPA1 and RHOB, but we could not quantify TSP1 or LAMB2. This could be explained by the restricted sensitivity of PRM assays for peptide detection in BAL (*e.g.* TSP1) or peptide absence in BAL (*e.g.* LAMB2). Given the usual infrastructure and expertise in clinical laboratories, our targeted proteomics assays could be implemented for clinical monitoring. In fact, similar targeted mass spectrometry-based methodology is routinely used to quantify proteins, metabolites and drug levels in the clinic [70].

We quantified the respective AngII-regulated peptides in BAL of patients with stable lung function, ALAD and CLAD. Interestingly, all AngII-regulated peptides correlated strongly with the presence of neutrophils in the BAL fluid and the majority of them correlated with CMV viraemia. Our proteins thus hold promise for identification of patients with lung allograft inflammation. Individual AngII-regulated peptide concentrations could not discriminate between CLAD and non-CLAD patients, at the time of bronchoscopy. In contrast, a classifier based on the combined peptide concentrations exhibited significantly improved diagnostic accuracy. This is interesting and potentially biologically important, as it suggests coordinated secretion of these peptides is relevant and supports the value of combining markers.

Even more interestingly, patients who developed CLAD within 1-year follow-up demonstrated higher concentrations of BST1, GLNA and RHOB proteins compared with patients who remained stable. LYPA1 protein also showed a trend towards higher concentration in the CLAD group. While individual peptide concentrations predicted development of CLAD with relatively good accuracy, a classifier based on combined peptide concentrations enabled prediction of CLAD status with an almost perfect accuracy of 97%. Our data clearly show that the classifiers based on combined peptide concentrations yielded improved diagnostic accuracy and predictive value compared with individual proteins. Numerous studies have harnessed artificial intelligence and machine learning algorithms for improvement of diagnosis, proactive disease monitoring and personalised medicine [71–73]. Nevertheless, reassessment of these classifiers in an independent validation cohort is needed and is under way.

Our study has several strengths. This highly translational approach furthered insights into the expression of the renin–angiotensin system in CLAD and enabled quantification of AngII-regulated proteins in BAL, which may represent promising biomarkers. We took advantage of a unique patient cohort of lung transplant recipients with archived tissue and BAL samples. We used a multimodal approach as we tested our hypothesis in tissue and in BAL, and employed different (including cutting-edge) techniques to confirm our observations (immunostaining, RT-qPCR, Western blotting and mass spectrometry). As the direct activity of the renin–angiotensin system is difficult to assess due to the short half-lives of angiotensin peptides, we combined the measurement of AngII receptors with AngII-regulated proteins to gain insight into renin–angiotensin system activity. Finally, using machine learning algorithms, we demonstrate that the combination of AngII-regulated peptides can diagnose CLAD and predict later development of CLAD with high accuracy.

Notwithstanding its strengths, our study has some limitations. In this cross-sectional study, causality cannot be determined. Future analyses of longitudinal BAL samples will determine the stability and reproducibility of AngII-regulated peptides. The selection of the control group is challenging in studies involving lung tissue. For instance, we cannot formally exclude the influence of smoking, neoplasia (donor lungs) or ischaemia (lobectomy samples) on the expression of renin–angiotensin system proteins and AngII-regulated peptides. Finally, in the future, we will validate these observations in a larger cohort of lung transplant recipients and study mechanisms *via in vitro* and mouse orthotopic lung transplantation models.

Acknowledgements: The authors would like to thank the Toronto Lung Transplant Program Biobank team (Toronto, ON, Canada) for helping with sample collection and retrieval as well as Paul Chartrand, manager of the Latner Thoracic Surgery Research Laboratories (Toronto, ON, Canada), for facilitating experiment logistics. The authors also appreciate the tremendous dedication and hard work of all students, research fellows and technicians who helped with lung tissue collection and processing, often at odd hours of the night: Matthew White, Sajad Moshkelgosha, Betty Joe, Gafoor Puthiyaveetil, Akihiro Takahagi, Mitsuaki Kawashima, Tatsuaki Watanabe, Christina Lam, Goodness Madu, Nadia Sachewsky, Daniel Vosoughi, Madalina Maxim, Kristen Bounstra, Yohei Taniguchi and Alexander Tigert. Special thanks to Stephen Juvet (University Health Network, Toronto, ON, Canada) for his input regarding the general design of the study, immunostaining and RT-qPCR experiments. Special thanks to Davor Brinc (University Health Network, Toronto, ON, Canada) for consultation on PRM troubleshooting.

Author contributions: G. Berra: clinical screening, cohort design, sample collection and organisation, immunostaining, qPCR, Western blotting, data analysis, writing of manuscript. S. Farkona: experimental design, mass spectrometry, Western blotting, data analysis, writing of manuscript. Z. Mohammed-Ali: mass spectrometry. M. Kotlyar: bioinformatic analyses, machine learning algorithms, help with manuscript writing. L. Levy: cohort design, collection and handling of samples, help with manuscript writing. S. Clotet-Freixas: Western blotting. P. Ly: immunostaining. B. Renaud-Picard: clinical screening, collection of samples, histological grading. G. Zehong: help with immunostaining protocols. T. Daigneault: collection of samples. A. Duong: collection and organisation of samples. I. Batruch: technical assistance with mass spectrometry. I. Jurisica: protein interactome generation, bioinformatic analyses supervision. A. Konvalinka and T. Martinu: conception of the research question, cohort design, experimental design, supervision of experiments, data analysis, manuscript writing and editing.

Conflict of interest: G. Berra has nothing to disclose. S. Farkona has nothing to disclose. Z. Mohammed-Ali has nothing to disclose. M. Kotlyar has nothing to disclose. L. Levy has nothing to disclose. S. Clotet-Freixas has nothing to disclose. P. Ly has nothing to disclose. B. Renaud-Picard has nothing to disclose. G. Zehong has nothing to disclose. T. Daigneault has nothing to disclose. A. Duong has nothing to disclose. I. Batruch has nothing to disclose. I. Jurisica reports grants and nonfinancial support (in-kind contribution to grants) from IBM, personal fees for lectures and other (reimbursement of expenses) from Novartis and Canadian Rheumatology Association, outside the submitted work. A. Konvalinka has nothing to disclose. T. Martinu reports grants from Canadian Donation and Transplantation Research Program and Di Pochi funds, during the conduct of the study; grants from Sanofi, nonfinancial support from APCBio, outside the submitted work.

Support statement: The authors disclose receipt of the following financial support for this research: Canadian National Transplant Research Program, Kidney Foundation of Canada Predictive Biomarker Grant, Canadian Institute for Health Research (CIHR), Kidney Research Scientist Core Education, National Training (KRESCENT) program, Di Pochi funds, Toronto General and Western Hospital Foundation, University Health Network Multi Organ Transplant Program, and Les Hôpitaux Universitaires de Genève. Computational analyses were supported in part by grants from the Ontario Research Fund (34876) and Canada Foundation for Innovation (29272, 225404 and 33536). Funding information for this article has been deposited with the Crossref Funder Registry.

References

1 Chambers DC, Cherikh WS, Harhay MO, *et al.* The International Thoracic Organ Transplant Registry of the International Society for Heart and Lung Transplantation: thirty-sixth adult lung and heart-lung transplantation report – 2019; focus theme: donor and recipient size match. *J Heart Lung Transplant* 2019; 38: 1042–1055.
2 Glanville AR, Verleden GM, Todd JL, *et al.* Chronic lung allograft dysfunction: definition and update of restrictive allograft syndrome – a consensus report from the Pulmonary Council of the ISHLT. *J Heart Lung Transplant* 2019; 38: 483–492.
3 Sato M, Waddell TK, Wagnetz U, *et al.* Restrictive allograft syndrome (RAS): a novel form of chronic lung allograft dysfunction. *J Heart Lung Transplant* 2011; 30: 735–742.
4 Royer PJ, Olivera-Botello G, Koutsokera A, *et al.* Chronic lung allograft dysfunction: a systematic review of mechanisms. *Transplantation* 2016; 100: 1803–1814.
5 Verleden SE, Todd JL, Sato M, *et al.* Impact of CLAD phenotype on survival after lung retransplantation: a multicenter study. *Am J Transplant* 2015; 15: 2223–2230.
6 Verleden SE, Ruttens D, Vandermeulen E, *et al.* Bronchiolitis obliterans syndrome and restrictive allograft syndrome: do risk factors differ? *Transplantation* 2013; 95: 1167–1172.
7 Verleden GM, Raghu G, Meyer KC, *et al.* A new classification system for chronic lung allograft dysfunction. *J Heart Lung Transplant* 2014; 33: 127–133.
8 Todd JL, Jain R, Pavlisko EN, *et al.* Impact of forced vital capacity loss on survival after the onset of chronic lung allograft dysfunction. *Am J Respir Crit Care Med* 2014; 189: 159–166.
9 Fernandez IE, Heinzelmann K, Verleden S, *et al.* Characteristic patterns in the fibrotic lung. Comparing idiopathic pulmonary fibrosis with chronic lung allograft dysfunction. *Ann Am Thorac Soc* 2015; 12: Suppl. 1, S34–S41.
10 Kennedy VE, Todd JL, Palmer SM. Bronchoalveolar lavage as a tool to predict, diagnose and understand bronchiolitis obliterans syndrome. *Am J Transplant* 2013; 13: 552–561.
11 Saito T, Liu M, Binnie M, *et al.* Distinct expression patterns of alveolar “alarmins” in subtypes of chronic lung allograft dysfunction. *Am J Transplant* 2014; 14: 1425–1432.
12 Zhang F, Liu H, Liu D, *et al.* Effects of RAAS inhibitors in patients with kidney disease. *Curr Hypertens Rep* 2017; 19: 72.
13 Sun N, Zhai L, Li H, *et al.* Angiotensin-converting enzyme inhibitor (ACEI)-mediated amelioration in renal fibrosis involves suppression of mast cell degranulation. *Kidney Blood Press Res* 2016; 41: 108–118.
14 Lewis EJ, Hunsicker LG, Bain RP, *et al.* The effect of angiotensin-converting-enzyme inhibition on diabetic nephropathy. *N Engl J Med* 1993; 329: 1456–1462.

15 Konigshoff M, Wilhelm A, Jahn A, *et al.* The angiotensin II receptor 2 is expressed and mediates angiotensin II signaling in lung fibrosis. *Am J Respir Cell Mol Biol* 2007; 37: 640–650.
16 Ruppert ADP, Capelozzi V, Parra ER. Overexpression of angiotensin II type 1 receptor (AGTR1) and lymphatic vasculature rarefaction is present in scleroderma with pulmonary compromised. *Eur Respir J* 2012; 40: Suppl. 56, P3643.
17 Bader M, Peters J, Baltatu O, *et al.* Tissue renin-angiotensin systems: new insights from experimental animal models in hypertension research. *J Mol Med* 2001; 79: 76–102.
18 Konvalinka A, Batruch I, Tokar T, *et al.* Quantification of angiotensin II-regulated proteins in urine of patients with polycystic and other chronic kidney diseases by selected reaction monitoring. *Clin Proteom* 2016; 13: 16.
19 Konvalinka A, Zhou J, Dimitromanolakis A, *et al.* Determination of an angiotensin II-regulated proteome in primary human kidney cells by stable isotope labeling of amino acids in cell culture (SILAC). *J Biol Chem* 2013; 288: 24834–24847.
20 Mohammed-Ali Z, Tokar T, Batruch I, *et al.* Urine angiotensin II signature proteins as markers of fibrosis in kidney transplant recipients. *Transplantation* 2019; 103: e146–e158.
21 Meltzer EB, Barry WT, D'Amico TA, *et al.* Bayesian probit regression model for the diagnosis of pulmonary fibrosis: proof-of-principle. *BMC Med Genom* 2011; 4: 70.
22 Chen Y, Wang X, Weng D, *et al.* A TSP-1 synthetic peptide inhibits bleomycin-induced lung fibrosis in mice. *Exp Toxicol Pathol* 2009; 61: 59–65.
23 Yehualaeshet T, O'Connor R, Begleiter A, *et al.* A CD36 synthetic peptide inhibits bleomycin-induced pulmonary inflammation and connective tissue synthesis in the rat. *Am J Respir Cell Mol Biol* 2000; 23: 204–212.
24 Safi R, Nelson ER, Chitneni SK, *et al.* Copper signaling axis as a target for prostate cancer therapeutics. *Cancer Res* 2014; 74: 5819–5831.
25 Huang X, Ji G, Wu Y, *et al.* LAMA4, highly expressed in human hepatocellular carcinoma from Chinese patients, is a novel marker of tumor invasion and metastasis. *J Cancer Res Clin Oncol* 2008; 134: 705–714.
26 Emblom-Callahan MC, Chhina MK, Shlobin OA, *et al.* Genomic phenotype of non-cultured pulmonary fibroblasts in idiopathic pulmonary fibrosis. *Genomics* 2010; 96: 134–145.
27 Xue H, Zhang G, Geurts AM, *et al.* Tissue-specific effects of targeted mutation of *Mir29b1* in rats. *EBioMedicine* 2018; 35: 260–269.
28 Cushing L, Kuang P, Lü J. The role of miR-29 in pulmonary fibrosis. *Biochem Cell Biol* 2015; 93: 109–118.
29 He Y, Huang C, Lin X, *et al.* MicroRNA-29 family, a crucial therapeutic target for fibrosis diseases. *Biochimie* 2013; 95: 1355–1359.
30 Pandit KV, Milosevic J, Kaminski N. MicroRNAs in idiopathic pulmonary fibrosis. *Transl Res* 2011; 157: 191–199.
31 Patel V, Noureddine L. MicroRNAs and fibrosis. *Curr Opin Nephrol Hypertens* 2012; 21: 410–416.
32 Zhou C, Moustafa MR, Cao L, *et al.* Modeling and multiscale characterization of the quantitative imaging based fibrosis index reveals pathophysiological, transcriptome and proteomic correlates of lung fibrosis induced by fractionated irradiation. *Int J Cancer* 2019; 144: 3160–3173.
33 Haston CK, Tomko TG, Godin N, *et al.* Murine candidate bleomycin induced pulmonary fibrosis susceptibility genes identified by gene expression and sequence analysis of linkage regions. *J Med Genet* 2005; 42: 464–473.
34 Levy L, Huszti E, Renaud-Picard B, *et al.* Risk assessment of chronic lung allograft dysfunction phenotypes: validation and proposed refinement of the 2019 International Society for Heart and Lung Transplantation classification system. *J Heart Lung Transplant* 2020; 39: 761–770.
35 R Core Team. R: A Language and Environment for Statistical Computing. Vienna, R Core Team, 2018.
36 Wickham H. ggplot2: Elegant Graphics for Data Analysis. New York, Springer-Verlag, 2016.
37 Bischl B, Lang M, Kotthoff L, *et al.* mlr: machine learning in R. *J Mach Learn Res* 2016; 17: 1–5.
38 Robin X, Turck N, Hainard A, *et al.* pROC: an open-source package for R and S+ to analyze and compare ROC curves. *BMC Bioinformat* 2011; 12: 77.
39 National Center for Atmospheric Research – Research Applications Laboratory. verification: Weather Forecast Verification Utilities. 2015. https://cran.r-project.org/package=verification Date last accessed: 20 March 2021.
40 Wang J, Chen L, Chen B, *et al.* Chronic activation of the renin-angiotensin system induces lung fibrosis. *Sci Rep* 2015; 5: 15561.
41 Uhal BD, Li X, Piasecki CC, *et al.* Angiotensin signalling in pulmonary fibrosis. *Int J Biochem Cell Biol* 2012; 44: 465–468.
42 Uhal BD, Kim JK, Li X, *et al.* Angiotensin-TGF-beta 1 crosstalk in human idiopathic pulmonary fibrosis: autocrine mechanisms in myofibroblasts and macrophages. *Curr Pharm Des* 2007; 13: 1247–1256.
43 Nikaido A, Tada T, Nakamura K, *et al.* Clinical features of and effects of angiotensin system antagonists on amiodarone-induced pulmonary toxicity. *Int J Cardiol* 2010; 140: 328–335.
44 Murphy AM, Wong AL, Bezuhly M. Modulation of angiotensin II signaling in the prevention of fibrosis. *Fibrogenesis Tissue Repair* 2015; 8: 7.

45 Maclean AA, Liu M, Fischer S, *et al.* Targeting the angiotensin system in posttransplant airway obliteration: the antifibrotic effect of angiotensin converting enzyme inhibition. *Am J Respir Crit Care Med* 2000; 162: 310–315.
46 Takeda H, Katagata Y, Hozumi Y, *et al.* Effects of angiotensin II receptor signaling during skin wound healing. *Am J Pathol* 2004; 165: 1653–1662.
47 Steckelings UM, Henz BM, Wiehstutz S, *et al.* Differential expression of angiotensin receptors in human cutaneous wound healing. *Br J Dermatol* 2005; 153: 887–893.
48 Tox U, Steffen HM. Impact of inhibitors of the renin–angiotensin–aldosterone system on liver fibrosis and portal hypertension. *Curr Med Chem* 2006; 13: 3649–3661.
49 Turu G, Balla A, Hunyady L. The role of β-arrestin proteins in organization of signaling and regulation of the AT1 angiotensin receptor. *Front Endocrinol* 2019; 10: 519.
50 Makita N, Iwai N, Inagami T, *et al.* Two distinct pathways in the down-regulation of type-1 angiotension II receptor gene in rat glomerular mesangial cells. *Biochem Biophys Res Commun* 1992; 185: 142–146.
51 Haack KK, Mitra AK, Zucker IH. NF-kappaB and CREB are required for angiotensin II type 1 receptor upregulation in neurons. *PLoS One* 2013; 8: e78695.
52 Nishida M, Fujinaka H, Matsusaka T, *et al.* Absence of angiotensin II type 1 receptor in bone marrow-derived cells is detrimental in the evolution of renal fibrosis. *J Clin Invest* 2002; 110: 1859–1868.
53 Gunther J, Kill A, Becker MO, *et al.* Angiotensin receptor type 1 and endothelin receptor type A on immune cells mediate migration and the expression of IL-8 and CCL18 when stimulated by autoantibodies from systemic sclerosis patients. *Arthritis Res Ther* 2014; 16: R65.
54 Silva-Filho JL, Caruso-Neves C, Pinheiro AA. Angiotensin II type-1 receptor (AT1R) regulates expansion, differentiation, and functional capacity of antigen-specific $CD8^+$ T cells. *Sci Rep* 2016; 6: 35997.
55 Lennon R, Byron A, Humphries JD, *et al.* Global analysis reveals the complexity of the human glomerular extracellular matrix. *J Am Soc Nephrol* 2014; 25: 939–951.
56 Zhou Y, Poczatek MH, Berecek KH, *et al.* Thrombospondin 1 mediates angiotensin II induction of TGF-beta activation by cardiac and renal cells under both high and low glucose conditions. *Biochem Biophys Res Commun* 2006; 339: 633–641.
57 Bige N, Shweke N, Benhassine S, *et al.* Thrombospondin-1 plays a profibrotic and pro-inflammatory role during ureteric obstruction. *Kidney Int* 2012; 81: 1226–1238.
58 Maimaitiyiming H, Zhou Q, Wang S. Thrombospondin 1 deficiency ameliorates the development of adriamycin-induced proteinuric kidney disease. *PLoS One* 2016; 11: e0156144.
59 Maluf DG, Dumur CI, Suh JL, *et al.* Evaluation of molecular profiles in calcineurin inhibitor toxicity post-kidney transplant: input to chronic allograft dysfunction. *Am J Transplant* 2014; 14: 1152–1163.
60 Lin Y, Manning PT, Jia J, *et al.* CD47 blockade reduces ischemia-reperfusion injury and improves outcomes in a rat kidney transplant model. *Transplantation* 2014; 98: 394–401.
61 Lario S, Bescós M, Campos B, *et al.* Thrombospondin-1 mRNA expression in experimental kidney transplantation with heart-beating and non-heart-beating donors. *J Nephrol* 2007; 20: 588–595.
62 Mas VR, Mas LA, Archer KJ, *et al.* Evaluation of gene panel mRNAs in urine samples of kidney transplant recipients as a non-invasive tool of graft function. *Mol Med* 2007; 13: 315–324.
63 Hadi R, Shin K, Reder N, *et al.* Utility of glutamine synthetase immunohistochemistry in identifying features of regressed cirrhosis. *Modern Pathol* 2020; 33: 448–455.
64 Inoue T, Liping H, Rosin DL, *et al.* Bone marrow stromal cell antigen-1 identified by RNA-Seq and ChIP-Seq is important for inducing renal ischemia-reperfusion injury and fibrosis. 2017. www.asn-online.org/education/kidneyweek/2017/program-abstract.aspx?controlId=2768342 Date last accessed: 20 March 2021.
65 Engel ME, Datta PK, Moses HL. RhoB is stabilized by transforming growth factor beta and antagonizes transcriptional activation. *J Biol Chem* 1998; 273: 9921–9926.
66 Vardouli L, Vasilaki E, Papadimitriou E, *et al.* A novel mechanism of TGFβ-induced actin reorganization mediated by Smad proteins and Rho GTPases. *FEBS J* 2008; 275: 4074–4087.
67 Drabovich AP, Dimitromanolakis A, Saraon P, *et al.* Differential diagnosis of azoospermia with proteomic biomarkers ECM1 and TEX101 quantified in seminal plasma. *Sci Transl Med* 2013; 5: 212ra160.
68 Hüttenhain R, Soste M, Selevsek N, *et al.* Reproducible quantification of cancer-associated proteins in body fluids using targeted proteomics. *Sci Transl Med* 2012; 4: 142ra194.
69 Karakosta TD, Soosaipillai A, Diamandis EP, *et al.* Quantification of human kallikrein-related peptidases in biological fluids by multiplatform targeted mass spectrometry assays. *Mol Cell Proteom* 2016; 15: 2863–2876.
70 Arora A, Somasundaram K. Targeted proteomics comes to the benchside and the bedside: is it ready for us? *Bioessays* 2019; 41: e1800042.
71 Richardson A, Signor BM, Lidbury BA, *et al.* Clinical chemistry in higher dimensions: machine-learning and enhanced prediction from routine clinical chemistry data. *Clin Biochem* 2016; 49: 1213–1220.
72 Gruson D, Helleputte T, Rousseau P, *et al.* Data science, artificial intelligence, and machine learning: opportunities for laboratory medicine and the value of positive regulation. *Clin Biochem* 2019; 69: 1–7.
73 Grapov D, Fahrmann J, Wanichthanarak K, *et al.* Rise of deep learning for genomic, proteomic, and metabolomic data integration in precision medicine. *OMICS* 2018; 22: 630–636.